Available online at www.sciencedirect.com
ScienceDirect
Engineering Structures 29 (2007) 1178–1188
ENGINEERING STRUCTURES
www.elsevier.com/locate/engstruct

Seismic retrofit of a reinforced concrete flat-slab structure: Part II — seismic fragility analysis

Mary Beth D. Hueste*, Jong-Wha Bai

Zachry Department of Civil Engineering, Texas A&M University, College Station, TX, USA

Received 12 April 2005; received in revised form 30 June 2006; accepted 7 July 2006
Available online 2 October 2006

Abstract

An assessment of seismic fragility was conducted for a reinforced concrete (RC) frame structure representative of 1980s construction in the Central United States. The performance of the unretrofitted structure is presented in terms of fragility relationships that relate the probability of exceeding a performance level to the earthquake intensity. In addition, seismic fragility relationships were developed for the retrofitted structure based on three possible retrofit techniques and several performance levels. Fragility curves for the retrofitted structure were compared with those for the unretrofitted structure.

For development of seismic fragility curves, the FEMA 356 global drift limits were compared with drift limits based on the FEMA 356 member-level criteria. In addition, a punching shear prediction model was used to establish an upper bound drift limit. Performance levels based on additional quantitative limits were also considered. Varying degrees of reduction in the seismic fragility were demonstrated through the use of the three selected retrofit techniques. The fragility curves were compared to those for RC structures derived in other studies and it was found that the results based on this study are comparable.

Keywords: Concrete, reinforced; Concrete slabs; Buildings; Retrofitting; Seismic analysis; Reliability

1. Introduction

Improved understanding of the dynamic behavior and seismic performance of structures has led to new advances in earthquake engineering in recent years. In particular, the performance-based design approach allows for selection of a specific performance objective based on various parameters, including the owner's requirements, the functional utility of the structure, the seismic risk, and potential economic losses. In spite of these recent advances, many structures in the Central United States (US) were not designed for any level of seismic resistance until after the 1989 Loma Prieta earthquake in San Francisco, California, and the 1994 Northridge, California, earthquake. The increased awareness of the presence of the New Madrid Seismic Zone in the Central US has led to a concern for the seismic vulnerability of structures in this area. It is important to evaluate these structures and determine ways to improve the seismic resistance of systems that are found to be vulnerable.

Recently, a number of research studies related to seismic vulnerability and the methodology of developing fragility curves have been actively conducted [1–8]. However, few studies have evaluated the seismic fragility of representative structures in the Central US.

Several intervention methods were evaluated for a typical 1980s reinforced concrete (RC) building in the Central US. Nonlinear analysis using synthetic ground motions recently developed for the region provides the structural response data used to derive fragility relationships that relate the probability of exceeding a particular performance level to earthquake intensity. Such relationships provide a useful tool for decision makers to evaluate the relative benefit of retrofitting structures as compared to other mitigation measures.

This is the second of two papers that focus on the seismic fragility of the retrofitted and unretrofitted case study structure. The first paper [9] describes the seismic performance evaluation for the unretrofitted and retrofitted case study structures. Additional details are documented in the research report [10].

* Corresponding author.
E-mail addresses: mhueste@tamu.edu (M.B.D. Hueste), jongwhabai@tamu.edu (J.-W. Bai).

0141-0296/$ - see front matter © 2006 Elsevier Ltd. All rights reserved.
doi:10.1016/j.engstruct.2006.07.022

2. Scope and research objective

The scope of this study is to assess the seismic fragility of a typical 1980s RC building in the Central US. In particular, the effectiveness of retrofitting was evaluated by estimating the reduction in the probability of exceeding a certain limit state, as compared to the unretrofitted structure. In addition, several different drift limits for the development of seismic fragility were evaluated.

A five-story flat-slab RC case study building with a moment frame system was used in this study. Performance levels were described in terms of drift limits based on the global-level and member-level limits found in the *Prestandard and commentary for the seismic rehabilitation of buildings* (FEMA 356) [11], along with additional quantitative drift limits based on the specific response characteristics of the structure. To develop the desired fragility curves, results from nonlinear time history analysis conducted with synthetic ground motion data were used. The fragility curves derived in this study were compared to those for RC structures found in the literature.

This study is part of a Mid-America Earthquake (MAE) Center research program focusing on consequence minimization, which contributes to the development of a new Consequence Based Engineering paradigm. The findings of this study provide information about the expected seismic performance of a common type of structure in Mid-America, as well as the potential to minimize the expected damage for varying earthquake intensities through retrofit.

3. Background

A five-story, reinforced concrete (RC) office building designed based on the code requirements used in the Central US region during the early 1980s was selected as a case study building. The case study building has a moment frame system not specially detailed for ductile behavior. The floor system is composed of a flat slab and perimeter moment resisting frames with spandrel beams. Design load requirements were taken from the ninth edition of the BOCA Basic/National Code [12] and the structural member design follows the provisions of the American Concrete Institute (ACI) Building code requirements for reinforced concrete, ACI 318-83 [13].

Several retrofit techniques were evaluated for the case study structure with a goal of modifying different structural response parameters, including stiffness, strength and ductility. The three selected techniques include addition of shear walls, addition of RC column jackets, and confinement of the column plastic hinge regions using externally bonded steel plates. More details for design requirements and analytical modeling of the unretrofitted and retrofitted case study building are found in the companion paper [9].

To develop the fragility curves, two sources of synthetic ground motion data were used [14,15]. The first set of ground motions are suites of synthetic records developed by Wen and Wu [14]. Each suite contains ten ground motions whose median response corresponds to the specified return rate and location. Return rates of 275 years (10% probability of exceedance in 50 years) and 2475 years (2% probability of exceedance in 50 years) were used for both St. Louis, Missouri, and Memphis, Tennessee. The other set of ground motions are suites of synthetic records for Memphis, Tennessee, developed by Rix and Fernandez-Leon [15], based on stochastic ground motion models. Two source models were considered in the development of these records, Atkinson and Boore [16] and Frankel et al. [17], to capture the impact of modeling uncertainty. Synthetic ground motion sets were developed for three body wave magnitudes (M 5.5, 6.5 and 7.5) and four hypocentral distances (10, 20, 50 and 100 km).

4. Fragility curve development

To develop the fragility curves, several parameters are needed, including structural response characteristics, earthquake intensities, and uncertainties for capacity and demand. The seismic demand was determined from the synthetic ground motion data developed by Wen and Wu [14] and Rix and Fernandez-Leon [15]. The desired fragility curves were developed using the following equation [18].

$$P(LS/S_a) = 1 - \Phi\left(\frac{\lambda_{CL} - \lambda_{D/S_a}}{\sqrt{\beta^2_{D/S_a} + \beta^2_{CL} + \beta^2_M}}\right) \quad (1)$$

where:

$P(LS/S_a)$ = Probability of exceeding a specified limit state given the spectral acceleration at the fundamental period of the building

Φ = Standard normal cumulative distribution function

λ_{CL} = ln (*median of drift capacity for a particular limit state*), where drift capacity is expressed as a percentage of the story height

λ_{D/S_a} = ln (*median calculated demand drift given the spectral acceleration*), where demand drift is determined from a fitted power law equation

β_{D/S_a} = Uncertainty associated with the fitted power law equation used to estimate demand drift = $\sqrt{\ln(1+s^2)}$

β_{CL} = Uncertainty associated with the drift capacity criteria, taken as 0.3 for this study [18]

β_M = Uncertainty associated with analytical modeling of the structure, taken as 0.3 for this study [18]

s^2 = Square of the standard error = $\frac{\sum[\ln(Y_i)-\ln(Y_p)]^2}{n-2}$

Y_i and Y_p = Observed demand drift and power law predicted demand drift, respectively, given the spectral acceleration

n = Number of sample data points for demand.

To demonstrate the methodology for derivation of the fragility curves, the unretrofitted case study building is considered using the FEMA 356 global-level drift limits and the synthetic ground motion records developed by Wen and Wu [14]. Fig. 1 provides the relationship between maximum interstory drift and the corresponding spectral acceleration for both the 10% in 50 years and the 2% in 50 years Wen and Wu motions developed for Memphis. A total of 20 points are plotted, where each data point represents the

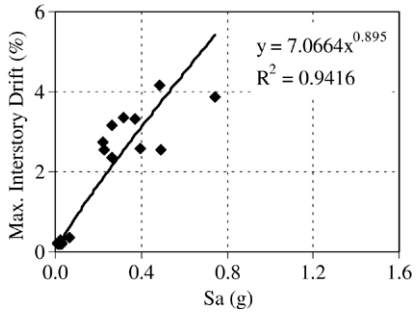

Fig. 1. Development of power law equation for unretrofitted structure (Wen and Wu Memphis motions).

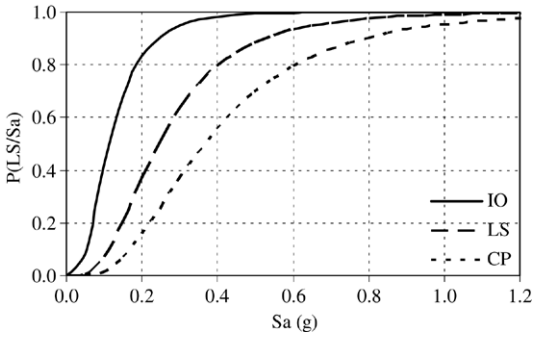

Fig. 2. Global-level fragility curves for unretrofitted structure (Wen and Wu Memphis motions).

Table 1
Interstory drift limits based on FEMA 356 global-level criteria (percent)

Structure	Drift limits (%)		
	IO	LS	CP
Concrete frame	1	2	4 (2.9[a])
Concrete wall	0.5	1 (0.85[b])	2 (1.2[b])

[a] Punching shear, CP limited to 2.9% versus 4% based on punching shear prediction.

[b] Shear wall failure, LS and CP limited to 0.85% and 1.2% versus 1% and 2% based on shear wall failure in shear.

demand relationship for one ground motion record. The spectral acceleration (S_a) for a given ground motion record is the value corresponding to the fundamental period of the structure based on cracked section properties ($T_1 = 1.62$ s) and 5% damping. The drift demand value is the maximum interstory drift determined during the nonlinear time history analysis of the structure when subject to that ground motion record. The best fit power law equation is also provided in the graph. This equation is used to describe the demand drift when constructing the fragility curves for the unretrofitted structure. The corresponding value of s^2 for the unretrofitted case is 0.114, which gives a β_{D/S_a} value of 0.328. The fragility curves for three limit states including Immediate Occupancy (IO), Life Safety (LS), and Collapse Prevention (CP) developed using the FEMA 356 global-level performance criteria are shown in Fig. 2. The corresponding drift limits for RC frame structures are provided in Table 1.

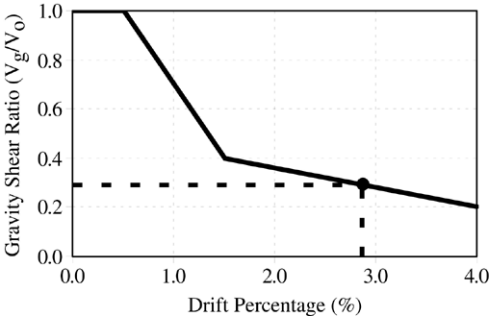

Fig. 3. Prediction model for punching shear and flexural punching shear failures at interior slab–column connections (adapted from Hueste and Wight [19]).

5. Limit state criteria for development of fragility curves

5.1. FEMA 356 global-level limits

An initial set of fragility curves was developed using the FEMA 356 global-level drift limits where the drift limit for each performance level (IO, LS and CP) is defined by a maximum interstory drift for a given type of structure. This approach may not be appropriate for predicting specific member-level performance. However, it is useful as a first approximation of structural behavior under seismic demands.

The median drift capacity term λ_{CL} for the fragility analysis was calculated as the natural log of the specified limiting interstory drift, expressed as a percentage of story height. Table 1 summarizes the drift limits used when developing fragility curves based on the FEMA 356 global-level criteria for the unretrofitted and retrofitted structures. The FEMA 356 global-level drift limits for concrete frame structures (1, 2 and 4%) were initially selected for the IO, LS, and CP performance levels, respectively.

The RC flat slab building is vulnerable to punching shear failure under significant lateral displacements during seismic loadings. For this reason, the punching shear prediction model based on the gravity shear ratio (V_g/V_o) and interstory drift proposed by Hueste and Wight [19] was used to establish an upper bound drift limit for CP. Fig. 3 shows the proposed relationship between interstory drift and the gravity shear ratio under seismic loads. For the case study building, V_g/V_o is 0.29 at the floor levels and 0.39 at the roof level. Because the maximum interstory drift occurred at the lower stories for the push-over and dynamic analyses, a gravity shear ratio of 0.29 was used to find the corresponding drift limit of 2.9% for prediction of punching shear failure at the interior floor slab–column connections, which is less than the 4% limit for CP given by FEMA 356. Therefore, 2.9% was used as the global drift limit for derivation of the CP fragility curve.

The drift limit for the concrete shear wall used as a retrofit measure was limited to 1.2% for CP based on shear failure of the wall. The corresponding reduced drift limit for the LS limit state (0.85%) was calculated as the average of the IO and CP drift limits.

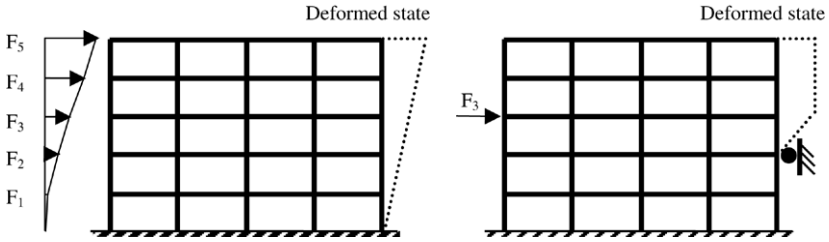

(a) Inverted triangular loading (first mode response).

(b) Critical third story response.

Fig. 4. Example loading patterns for push-over analysis.

Table 2
Interstory drift limits based on FEMA 356 member-level and additional quantitative limits (percent)

Structure	FEMA 356 global			FEMA 356 member (Regular push-over)			FEMA 356 member (Critical response push-over)			Additional quantitative		
	IO	LS	CP	IO	LS	CP	IO	LS	CP	FY	PMI	SD
Unretrofitted	1	2	2.9[a]	0.88	0.88	1.07	0.62	0.62	0.69	0.36	0.66	2.81
Retrofit 1	0.5	0.85[b]	1.2[b]	0.4[c]	0.6[c]	0.75[c]	0.4[c]	0.6[c]	0.75[c]	0.74	1.2[d]	–
Retrofit 2	1	2	2.9[a]	0.96	1.29	1.29	0.88	1.37	1.37	0.53	1.23	–
Retrofit 3	1	2	2.9[a]	1.07	1.74	1.89	0.83	1.46	1.81	0.55	0.79	–

[a] Drift limits for CP limited to 2.9% versus 4% based on punching shear prediction.
[b] Drift limits for LS and CP limited to 0.85% and 1.2% versus 1% and 2% based on shear wall failure in shear.
[c] Drift limits governed by the FEMA 356 member-level criteria for shear wall members in Table 2.8 [11].
[d] PMI limited to 1.2% based on shear wall failure in shear.

5.2. FEMA 356 member-level limits

The global-level approach provides a general assessment of the seismic performance of a structure. However, it does not identify individual member deficiencies and does not consider specific member detailing. The FEMA 356 member-level criteria are given as member plastic rotation limits. To develop fragility curves based on the FEMA 356 member-level criteria, drift limits corresponding to the plastic rotation criteria were determined. In this study, two different analyses were used for determining the most critical interstory drift corresponding to the member-level criteria: (1) standard push-over analysis using an inverted triangular load pattern corresponding to the first mode, and (2) story-by-story push-over analysis used to find the critical interstory drift based on the development of a plastic mechanism within a story, as suggested by Dooley and Bracci [20].

Fig. 4 shows a comparison between a regular push-over analysis and a critical-response push-over analysis. As shown in Fig. 4(b), to determine the drift capacity of a story, the in-plane deformation of the level below is restrained to create the most critical story mechanism. The drift limits corresponding to the FEMA 356 member-level criteria are summarized in Table 2 for the unretrofitted and retrofitted structures.

5.3. Quantitative limits

In addition to the FEMA 356 global-level and member-level criteria for the IO, LS and CP performance levels, quantitative limit states were evaluated based on limits described by Wen et al. [8], as follows.

(1) First Yield (FY) — Interstory drift at which a member of a story or a structure initiates yielding under an imposed lateral loading.

(2) Plastic Mechanism Initiation (PMI) — Interstory drift at which a story mechanism (typical of a column sidesway mechanism), an overall beam sidesway mechanism, or a hybrid mechanism initiates under an imposed lateral loading.

(3) Strength Degradation (SD) — Interstory drift at which the story strength (resistance) has degraded by more than a certain percentage of the maximum strength (taken as 20% in this study). Note that strength degradation can occur due to material nonlinearities in the analytical models and also due to geometric nonlinearities from P-delta effects.

To develop fragility curves based on the additional quantitative limit states, the story-by-story push-over analysis suggested by Dooley and Bracci [20] was used to find the most critical interstory drift. The corresponding drift limits for each of the above quantitative limit states are provided in Table 2. In this case, the SD limit state was not detected for the retrofitted structure because the strength did not fall to 20% of the maximum strength.

6. Seismic fragility analysis using Wen and Wu motions

The initial seismic fragility analysis was conducted using the Wen and Wu Memphis motions. These motions were scaled by Wen and Wu such that the median demand matches the 2% and 10% probabilities of exceedance in 50 years events.

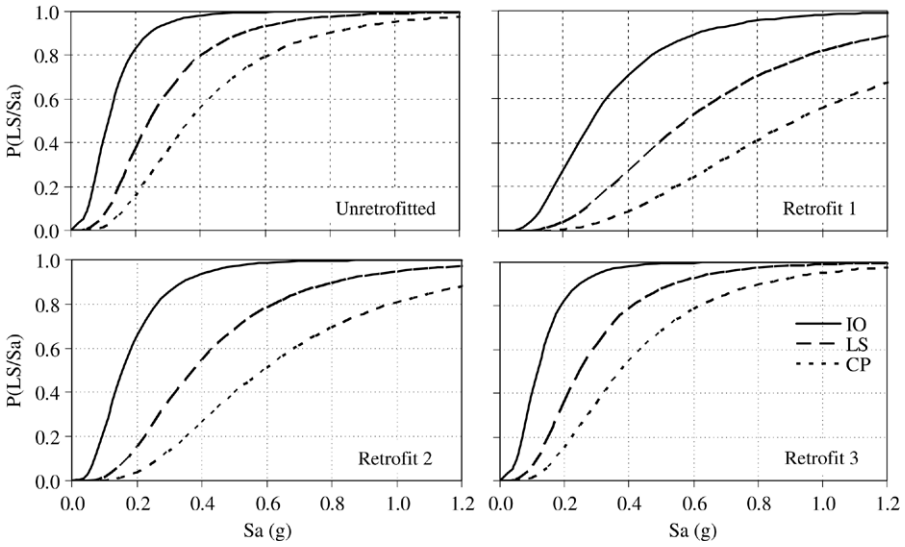

Fig. 5. Fragility curves based on FEMA 356 global-level limits (Wen and Wu Memphis motions).

6.1. FEMA 356 global-level limits

Fig. 5 shows the fragility curves derived using the FEMA 356 global-level limits for the unretrofitted and retrofitted structure. As shown, the probabilities of exceeding each limit state (IO, LS and CP) were reduced by the addition of shear walls (Retrofit 1) and RC column jackets (Retrofit 2). However, the fragility curves for the confinement of column plastic hinge zones (Retrofit 3) are the same as for the unretrofitted structure. The fragility curves are not modified by Retrofit 3 because the same global-level drift limits are used and the demand drifts are nearly the same since the added confinement does not modify the global structural response.

The spectral acceleration of concern can vary when the structure is retrofitted and so a direct comparison for a specific spectral acceleration may not be appropriate. Therefore, the impact of the retrofits on the fragility curves for each limit state are provided in Fig. 6 using peak ground acceleration (PGA) on the horizontal axis. Retrofit 1 reduced the probabilities of exceeding each limit state for PGA values above $0.25g$. Retrofit 2 reduced the fragility for each limit state and Retrofit 3 gives the same fragility as the unretrofitted structure.

6.2. FEMA 356 member-level limits

As shown in Table 2, the drift limits for regular push-over analysis are less stringent in most cases than those determined using a critical response (story-by-story) push-over analysis. For further analysis, the drift limits based on the critical response push-over analysis were used for the FEMA 356 member-level limits. Fig. 7 shows the fragility curves based on the FEMA 356 member-level limits for the unretrofitted and retrofitted structure.

Fig. 8 shows a comparison of the fragility curves with PGA on the horizontal axis. Retrofit 1 (shear walls) and Retrofit 3 (confinement of column ends) have a minimal impact on IO, but are effective in reducing the fragility for LS and CP, especially for PGA values up to $0.4g$. Retrofit 2 (column jacketing) provides the largest reduction in fragility for IO and LS of the three retrofits and provides a comparable reduction in fragility for CP.

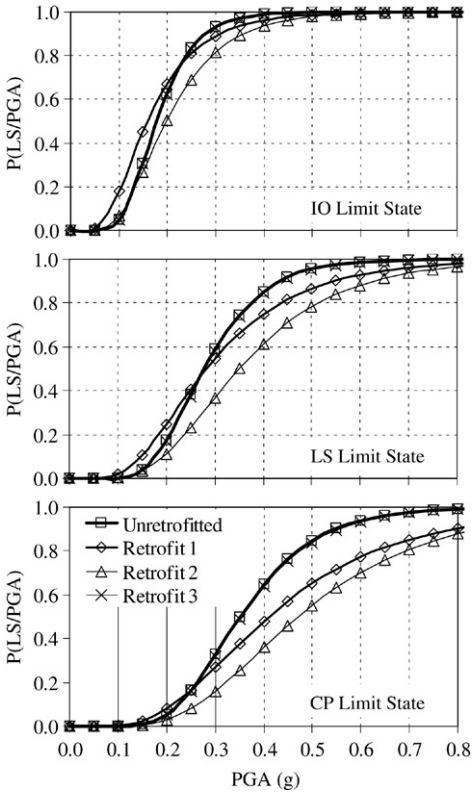

Fig. 6. Comparisons of fragility curves based on FEMA 356 global-level limits (Wen and Wu Memphis motions).

6.3. Quantitative limits

Fragility curves were developed for the FY and PMI limit states using the drift limits determined from the critical response (story-by-story) push-over analysis. Fig. 9 shows the fragility curves for the FY and PMI limit states for the

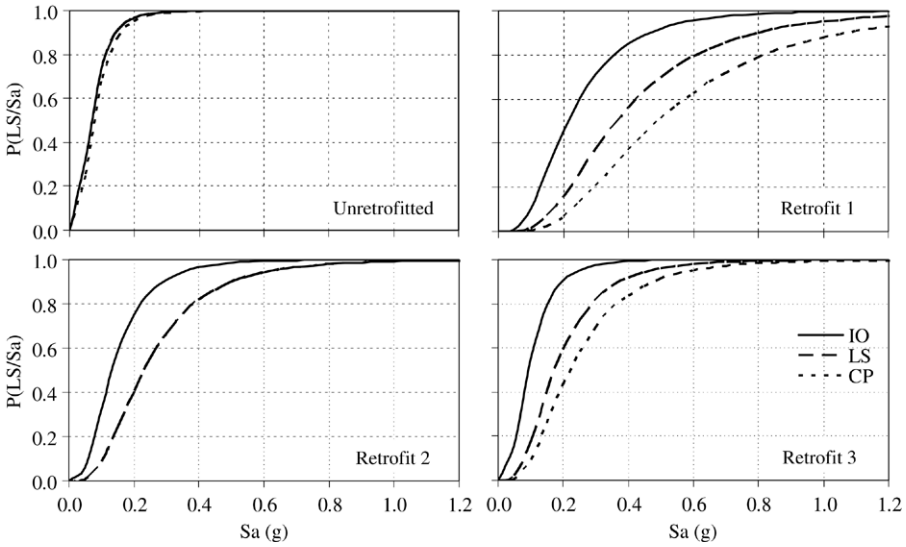

Fig. 7. Fragility curves based on FEMA 356 member-level limits (Wen and Wu Memphis motions).

unretrofitted and retrofitted structure. The fragilities for both limit states were reduced to varying degrees depending on the retrofit technique, limit state and magnitude of the spectral acceleration.

Fig. 10 shows the corresponding fragility curves for FY and PMI with PGA on the horizontal axis. Retrofit 1 (shear walls) gave the most significant reduction in fragility for these limit states. Retrofit 2 (column jacketing) gave a modest reduction in fragility for FY and a more substantial reduction in fragility for PMI. Retrofit 3 (confinement of column ends) gave only a small reduction in fragility for both limit states.

7. Seismic fragility analysis using Rix and Fernandez-Leon motions

The Memphis synthetic ground motions developed by Rix and Fernandez-Leon [15] for a 20 km hypocentral distance were used to derive additional fragility curves. The ground motions based on both source models (Atkinson and Boore [16] and Frankel et al. [17]) were used. The resulting fragility curves using the FEMA 356 global-level drift limits, with modifications for shear failures, are provided in Fig. 11. The results from the M 7.5 Frankel et al. motions for the unretrofitted, Retrofit 2 and Retrofit 3 cases are not included because the seismic evaluation indicated that the maximum interstory drift values were unreasonably high within some stories of the structure [9].

Fig. 12 shows the global-level fragility curves for the unretrofitted and retrofitted structures with the PGA as the earthquake intensity parameter on the horizontal axis. As shown in Fig. 12, the probabilities of exceeding each limit state were reduced to some degree by Retrofits 1 and 2, while the values for Retrofit 3 match the unretrofitted structure.

Fig. 13 shows the reduction in the probabilities exceeding each limit state when applying each of the three retrofits to the case study building. In general, a more significant reduction in seismic fragility is observed for each limit state when using the

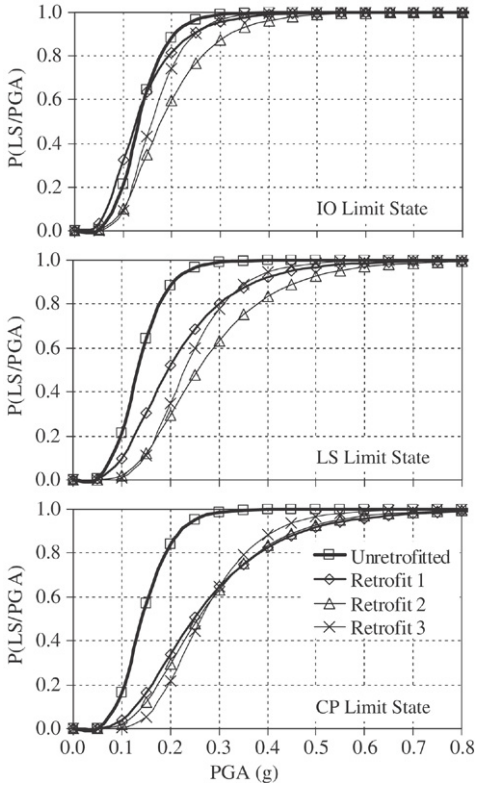

Fig. 8. Comparison of fragility curves based on FEMA 356 member-level limits (Wen and Wu Memphis motions).

FEMA 356 member-level limits and the additional quantitative limits as compared to the FEMA 356 global-level limits. Retrofit 1 (shear walls) gives the most substantial reduction in the seismic fragility for the FY and PMI limit states.

The fragility curves for the unretrofitted structure based on both ground motion sets are compared in Fig. 14. As shown, the fragility curves developed using Rix and Fernandez-Leon (RF) motions give slightly lower probabilities of exceedance for each limit state as compared to the fragility curves based on the Wen

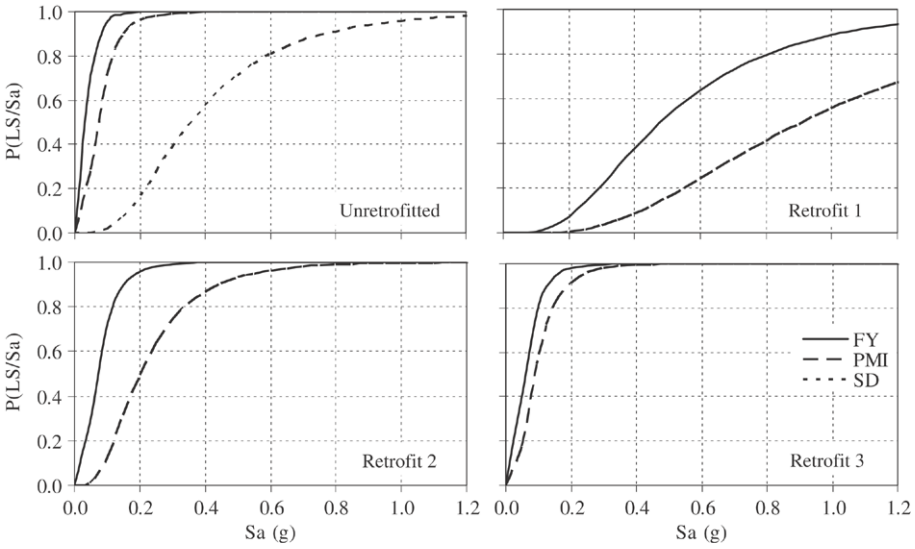

Fig. 9. Fragility curves based on additional quantitative limits (Wen and Wu Memphis motions).

and Wu (WW) motions. However, the fragility curves for the two different ground motion sets are not significantly different for each performance level evaluated. Based on a comparison of the two sets of fragility curves, the largest difference in the corresponding probability of exceedance values (the vertical dimension between corresponding curves at a certain spectral acceleration) occurs for the FY limit state.

8. Additional fragility curve comparisons

8.1. General

The fragility curves from this study based on the Rix and Fernandez-Leon motions were compared to those for RC frame structures found in the literature. The curves derived using the FEMA 356 global-level drift limits were selected for this comparison because the drift limits corresponding to the FEMA 356 member-level criteria and additional quantitative limits are more specific to the case study structure.

8.2. Fragility curves developed by Wen et al.

A three-story RC frame structure that was designed for gravity loads only and located in an area of low-to-moderate seismicity was selected for comparison [8]. The synthetic ground motions for Memphis developed by Wen and Wu [14] were used for the development of the fragility curves, along with the FEMA 356 global-level interstory drift limits of 1, 2, and 4% for the IO, LS and, CP limit states. The same value of modeling uncertainty ($\beta_M = 0.3$) was used. The fundamental period of the building for Wen et al. model was 0.87 s, which is smaller than that of the case study building (1.62 s based on the cracked section properties). Fig. 15(a) shows the comparison of fragility curves determined for the two studies. The seismic fragility curves for the IO, LS and CP limit states are relatively similar except for the slope.

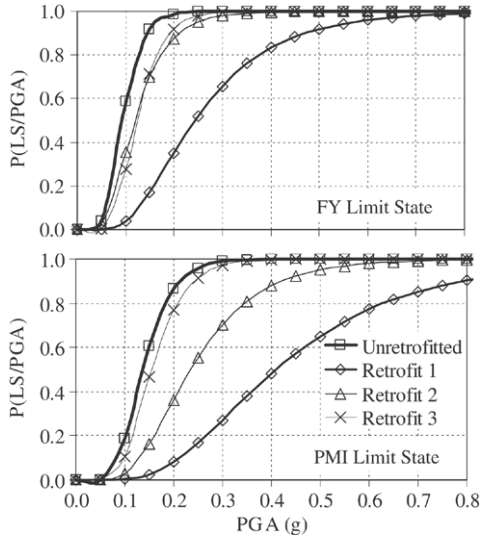

Fig. 10. Comparisons of fragility curves based on additional quantitative limits (Wen and Wu Memphis motions).

8.3. HAZUS fragility curves

Another comparison of fragility curves was made with those in the HAZUS 99 (SR2) technical report [21]. HAZUS is a software tool for assessing earthquake risk developed by the Federal Emergency Management Agency (FEMA) in agreement with the National Institute of Building Sciences. Fragility curves for four damage states including Slight damage (S), Moderate damage (M), Extensive damage (E), and Complete damage (C) were developed for HAZUS. The HAZUS low-code design level and mid-rise concrete moment frame structure (C1M) criteria were selected as parameters representing the unretrofitted case study structure.

Fig. 15(b) shows the comparison between the fragility curves based on the HAZUS methodology and those for the unretrofitted structure in this study. Because HAZUS uses spectral displacement (S_d) as a parameter of earthquake

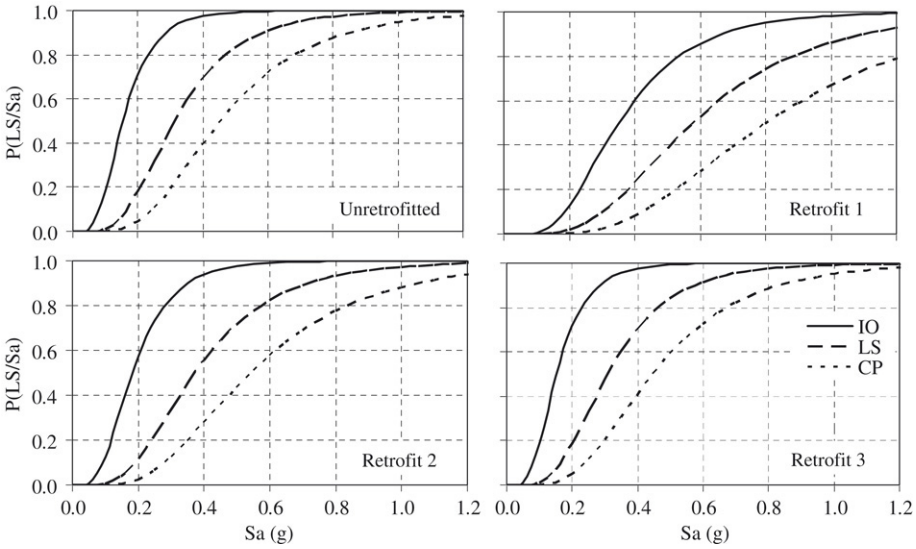

Fig. 11. Fragility curves based on FEMA 356 global-level limits (Rix and Fernandez-Leon motions).

intensity, the fragility curves from this study were modified to use S_d on the horizontal axis for comparison. As shown in Fig. 15(b), the HAZUS curves for the M and E damage states are comparable with the curves representing the IO and LS limit states for this study, respectively. The CP fragility curve gives higher probabilities of exceedance than the HAZUS C damage state. This is likely due the lower drift limits used in this study for CP based on the punching shear failure prediction model.

8.4. Fragility curves developed by Erberik and Elnashai

A five-story RC flat-slab structure infilled with masonry walls located in the Mid-America region was used for the last fragility curve comparison [22]. This building structure was designed using ACI 318-99 [23] and ten recorded ground motions were used for the development of fragility curves. The damage states used in the HAZUS methodology were selected for this research with spectral acceleration as the earthquake intensity parameter.

Fig. 15(c) shows the comparison of the seismic fragility curves. As shown, the fragility curves developed by Erberik and Elnashai provide lower probabilities of exceedance for comparable damage states. In fact, all damage states, with the exception of S, have lower fragilities than CP for the case study building. This can likely be attributed to the use of masonry infill walls in the structure studied by Erberik and Elnashai, which results in a structure that is much stiffer than the case study building.

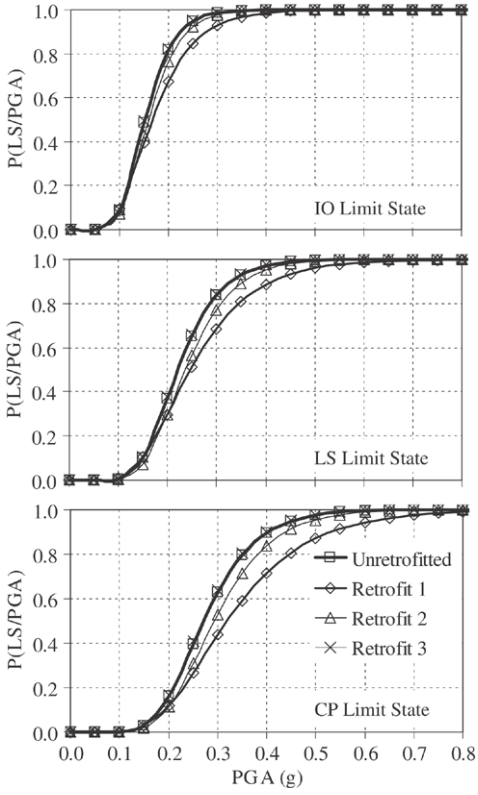

Fig. 12. Comparisons of fragility curves based on FEMA 356 global-level limits (Rix and Fernandez-Leon motions).

9. Summary and conclusions

Seismic fragility analysis for a five-story reinforced concrete (RC) flat-slab building representative of 1980s construction in the Mid-America region was conducted. Three retrofit techniques were applied to the case study structure to enhance the seismic performance, including addition of shear walls, addition of RC column jackets, and confinement of the column plastic hinge regions using externally bonded steel plates [9] and the impact of retrofit was assessed in terms of the seismic fragility. The following conclusions were made based on the results of this study.

1. The drift limits corresponding to the FEMA 356 member-level plastic rotation limits were determined using standard push-over analysis techniques and critical response (story-by-story) push-over analysis. The drift limits based on FEMA 356 member-level criteria tended to be significantly smaller than the FEMA 356 global-level limits. This is

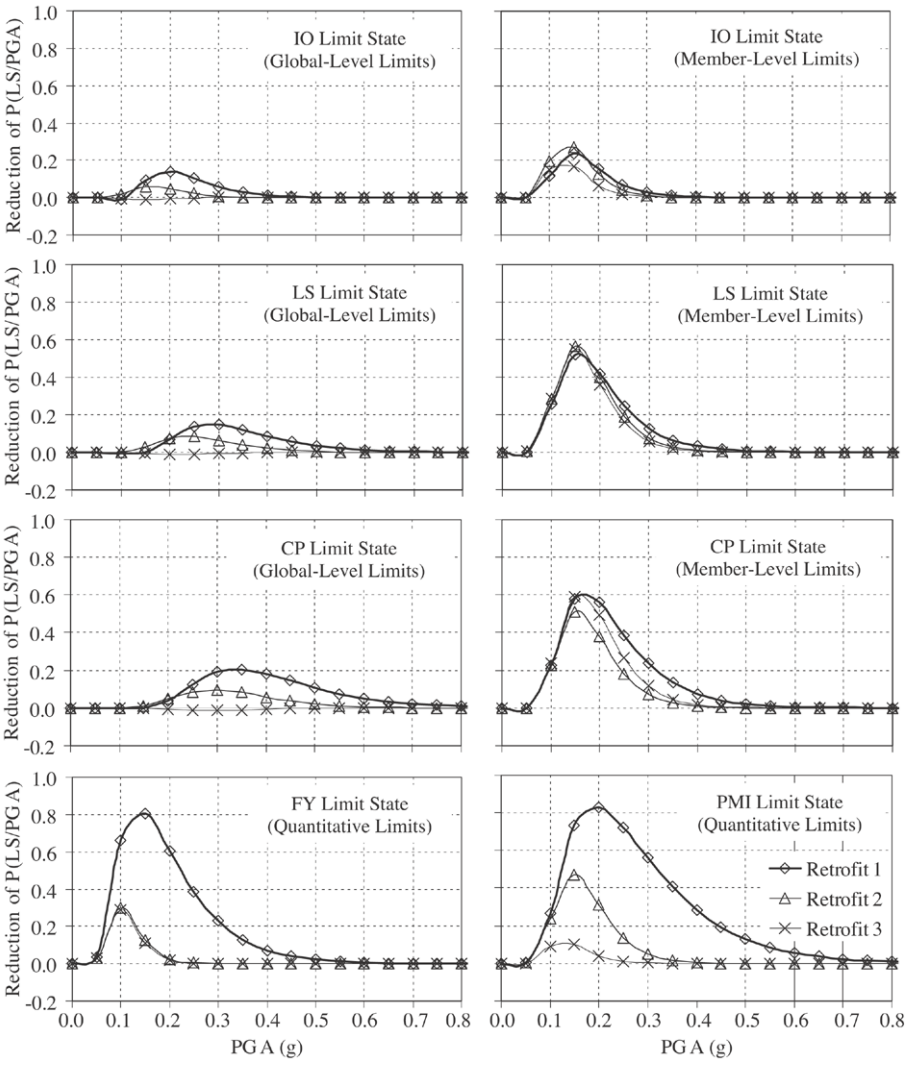

Fig. 13. Reduction of probabilities of exceeding each limit state (Rix and Fernandez-Leon motions).

because the member-level criteria better reflect the lack of seismic detailing and design for older Central US structures, whereas the FEMA 356 global-level (drift) limits are intended for well-detailed buildings. As a result, the probabilities of exceeding each limit state based on the FEMA 356 member-level drift limits tend to be higher than those based on the global-level drift limits.

2. Because the spectral acceleration of concern can vary when the structure is retrofitted, peak ground acceleration (PGA) was used for comparisons with the unretrofitted and retrofitted structures. The seismic fragility curves based on the FEMA 356 global-level criteria indicate that the addition of shear walls reduced the probabilities of exceeding each performance level [Immediate Occupancy (IO), Life Safety (LS) and Collapse Prevention (CP)] for PGA values above $0.25g$. RC column jackets reduced the probability of exceeding each performance levels. However, confining column plastic hinge zones with steel plates gave the same fragility as the unretrofitted structure.
3. Fragility curves developed using the FEMA 356 member-level criteria indicate that the use of shear walls and confinement of the column ends have a minimal impact on IO, but are effective in reducing the fragility for LS and CP, especially for PGA values up to $0.4g$. The column jacketing retrofit provides the largest reduction in fragility for IO and LS of the three retrofits and provides a comparable reduction in fragility for CP.
4. For the additional quantitative drift limits, the addition of shear walls gave the most significant reduction in fragility for the First Yield (FY) and Plastic Mechanism Initiation (PMI) limit states. The use of column jacketing gave a modest reduction in fragility for FY and a more substantial reduction in fragility for PMI. Use of confinement of the column ends gave only a small reduction in fragility for both limit states.
5. The fragility curves developed using the Wen and Wu motions and Rix and Fernandez-Leon motions were compared for the unretrofitted case study structure. The fragility curves based on the Rix and Fernandez-Leon motions tend to be less conservative for each limit state.
6. The fragility curves for the unretrofitted cases study building were compared to those from several other studies.

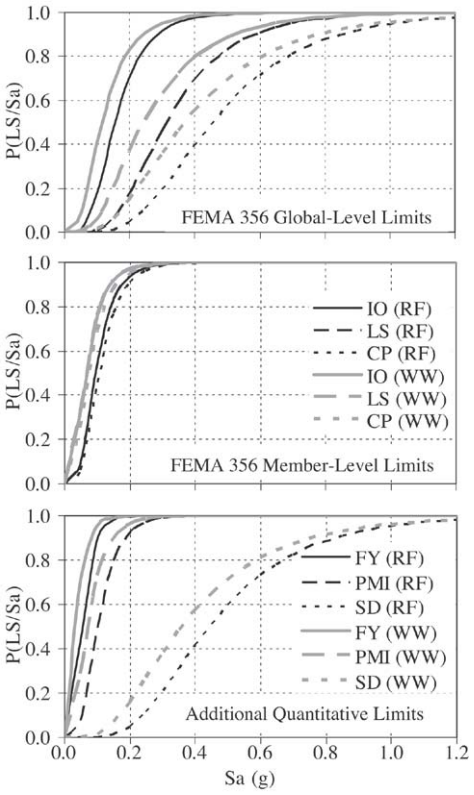

Fig. 14. Comparisons of fragility curves for the unretrofitted structure (Wen and Wu vs. Rix and Fernandez-Leon motions).

The comparison indicated that the fragility curves have reasonable agreement with a three-story RC moment frame structure and a HAZUS low-code design level mid-rise RC moment frame structure. Relatively poor comparison was found with fragility curves for a five-story RC flat-slab structure with masonry infill walls, which is likely due to the inherent differences in behavior for the two structure types.

It should be noted that the seismic fragility curves derived in this study provide important data for quantifying the vulnerability of existing structures in the Central United States. However, these fragility curves are representative of this particular case study structure and the selected retrofit techniques. Additional studies are needed to characterize the expected seismic fragility of vulnerable structures with different seismic response characteristics and to assess the effectiveness of retrofit techniques in reducing the seismic vulnerability of those structures. This is the second of two papers that focus on the seismic fragility of the retrofitted and unretrofitted case study structure. The first paper [9] describes the seismic performance evaluation for the unretrofitted and retrofitted case study structures.

Acknowledgments

The authors wish to acknowledge the National Science Foundation and the University of Illinois who funded this research through the Mid-America Earthquake Center (NSF Grant Number EEC-9701785). The financial support provided by the Civil Engineering Department at Texas A&M University, where this research was conducted, is also appreciated. The opinions expressed in this paper are those of the authors and do not necessarily reflect the views or policies of the sponsors.

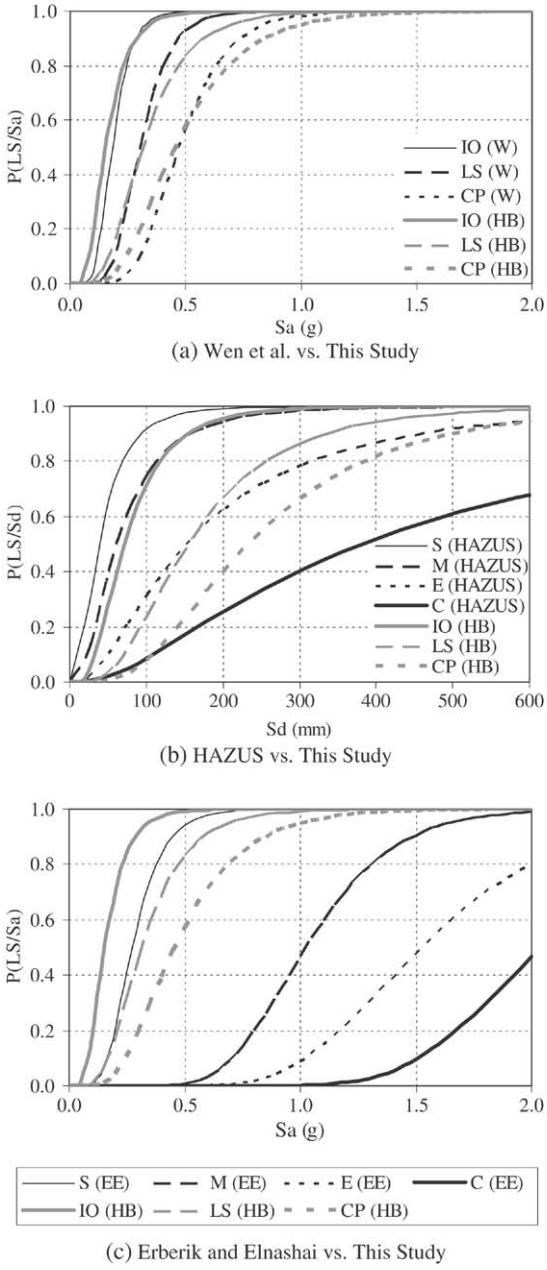

Fig. 15. Comparisons of fragility curves.

References

[1] Hassan AF, Sozen MA. Seismic vulnerability assessment of low-rise buildings in regions with infrequent earthquakes. ACI Structural Journal 1997;94(1):31–9.

[2] Gulkan P, Sozen MA. Procedure for determining seismic vulnerability of building structures. ACI Structural Journal 1999;96(3):336–42.

[3] Shinozuka M, Feng MQ, Lee J, Naganuma T. Statistical analysis of fragility curves. Journal of Engineering Mechanics 2000;126(12): 1224–31.

[4] Shinozuka M, Feng MQ, Kim H-K, Kim S-H. Nonlinear static procedure for fragility curve development. Journal of Engineering Mechanics 2000; 126(12):1287–95.
[5] Dumova-Jovanoska E. Fragility curves for reinforced concrete structures in Skopje (Macedonia) regions. Soil Dynamics and Earthquake Engineering 2000;19:455–66.
[6] Shama AA, Mander JB, Chen SS. Seismic investigation of steel pile bents: II. Retrofit and vulnerability analysis. Earthquake Spectra 2002;18(1): 143–60.
[7] Reinhorn AM, Barron-Corverra R, Ayala AG. Global spectral evaluation of seismic fragility of structures. In: Proc., 7th US national conference on earthquake engineering. 2002.
[8] Wen YK, Ellingwood BR, Veneziano D, Bracci JM. Uncertainty modeling in earthquake engineering. Mid-America earthquake center project FD-2 report. Urbana (IL): 2003.
[9] Hueste MD, Bai J-W. Seismic retrofit of a reinforced concrete flat-slab structure: Part I — Seismic performance evaluation. Engineering Structures 2007;29(6):1165–77.
[10] Bai J-W, Hueste MD. Deterministic and probabilistic evaluation of retrofit alternatives for a five-story flat-slab RC building. Mid-America earthquake center project CM-4 report. Urbana-Champaign (IL): Mid-America Earthquake Center, University of Illinois; 2006 [submitted for review].
[11] ASCE. Prestandard and commentary for the seismic rehabilitation of buildings (FEMA 356). Prepared by American society of civil engineers for the federal emergency management agency. Washington (DC); 2000.
[12] BOCA. Building officials and code administrators basic/national code/1984. Country Club Hills (IL): Building Officials and Code Administrators International, Inc; 1984.
[13] ACI Committee 318. Building code requirements for reinforced concrete (ACI 318-83). Detroit (MI): American Concrete Institute; 1983.
[14] Wen YK, Wu CL. Generation of ground motions for Mid-America cities. Mid-America Earthquake Center. http://mae.ce.uiuc.edu/newsite/research/rr-1/gmotions/index.html; January 2000.
[15] Rix GJ, Fernandez-Leon A. Earthquake ground motion simulation. http://www.ce.gatech.edu/research/mae_ground_motion/; September 2004.
[16] Atkinson G, Boore D. New ground motions relations for eastern North America. Bulletin of the Seismological Society of America 1995;85: 17–30.
[17] Frankel A, Mueller C, Barnhard T, Perkins D, Leyendecker E, Dickman N et al. National seismic hazard maps: Documentation. USGS open-file report 96-532. 1996.
[18] Wen YK, Ellingwood BR, Bracci JM. Vulnerability function framework for consequence-based engineering. Mid-America earthquake center project DS-4 report. Urbana (IL); 2004.
[19] Hueste MD, Wight JK. Nonlinear punching shear failure model for interior slab–column connections. Journal of Structural Engineering 1999; 125(9):997–1008.
[20] Dooley KL, Bracci JM. Seismic evaluation of column-to-beam strength ratios in reinforced concrete frames. ACI Structural Journal 2001;98(6): 843–51.
[21] FEMA. HAZUS 99 (SR2) technical report. Washington (DC): Federal Emergency Management Agency. 2002.
[22] Erberik MA, Elnashai AS. Fragility analysis of flat-slab structures. Engineering Structures 2004;26:937–48.
[23] ACI Committee 318. Building code requirements for reinforced concrete (ACI 318-99). Detroit (MI): American Concrete Institute; 1999.